Phase-dependent effects in multiphoton ionization induced by a laser field and its second harmonic

Kenneth J. Schafer and Kenneth C. Kulander
Physics Department, Lawrence Livermore National Laboratory, Livermore, California 94550
(Received 7 November 1991)

We present calculations of ionization rates, angular distributions, and above-threshold-ionization spectra for a hydrogen atom in a strong, two-color laser field. The two lasers are first- and second-harmonic fields with the same intensity and a constant relative phase difference between them. At longer wavelengths (1064 nm) and higher intensities ($> 10^{13}$ W/cm^2), there is clear evidence in the phase dependence of the ionization rates that ionization takes place primarily through tunneling. Even though the total ionization rate in this regime depends only on the peak value of the time-dependent electric field, the angular distributions show additional phase-sensitive effects. In particular, there is a large forward-backward asymmetry in the emitted electron distributions that is not simply correlated with the maximum electric field. At shorter wavelengths and/or lower intensities, there is a transition to multiphoton ionization with interference between ionization paths from the two lasers evident in the total ionization rates. In all cases, we find that the total ponderomotive shift of the ionization limit is the sum of the shifts for the two individual fields.

PACS number(s): 32.80.Rm

INTRODUCTION

The multiphoton ionization of atoms by the application of two strong lasers of different frequencies has attracted both experimental [1–4] and theoretical [5–7] interest in recent years. These two-color experiments and calculations have as their aim both the study of various features now familiar in multiphoton ionization, such as above-threshold ionization (ATI), and the investigation of new effects due to the simultaneous interaction of two different laser fields with the same atom. Additional interest has risen from the notion that the application of more than one cw laser might be an efficient way to implement "coherent control" of chemical reactions involving photodissociation [8].

Initially, two-color experiments were performed with the intention of studying the ponderomotive shift of an atom's ionization limit induced when a long-wavelength field is present. Ionization was separated from ponderomotive shifting by using a strong, long-wavelength laser to shift the ionization potential and a second, weaker and shorter-wavelength laser to actually ionize the atom. Trainham *et al.* [9] studied the photodetachment of Cl^- by a weak ultraviolet field in a strong low-frequency field. They found the size of the ponderomotive shift to be much smaller than expected. A similar experiment measuring the nonresonant ac Stark shifts of various Rydberg states [2] carried out with xenon, again found a smaller shift than expected. Attempts to model these experiments were largely unsuccessful [5,7]; the predicted shifts in the nonresonant ionization profiles were larger than the measured shifts, by a factor of 2 to 4.

Other experiments have focused on fields that are commensurate in the sense that one frequency is a harmonic of the other. Several groups have observed interference effects between a fundamental field and its third harmonic. Chen and Elliott [4] used this process to demonstrate the capability for measuring phase variations between optical transition amplitudes. Our interest in this area was stimulated by the recent experiments of Muller *et al.* [3], who studied ATI spectra from krypton atoms ionized by a 1064-nm laser and its second harmonic of 532 nm. In these experiments the lasers had the same intensity and a specified (variable) phase difference between them, giving a time-varying field of the form

$$\varepsilon(t)=\varepsilon_0[\sin(\omega t)+\sin(2\omega t+\phi)] \ . \tag{1}$$

Both fields were linearly polarized along the same axis and strong enough to be treated classically. (Note that our definition of the phase differs by $\pi/2$ from the convention in Ref. [3].) Muller *et al.* [3] found that the ionization rate as well as the relative widths and intensities of the ATI peaks depended on the intensity and relative phase of the two lasers. Fields of the form in Eq. (1) can lead to very asymmetric ionization processes, ejecting electrons in the forward or backward direction preferentially, depending upon the phase difference between the lasers. Ionization can also be observed with differing peak field strengths but the same ionization potential since the peak instantaneous value of the time-varying electric field in Eq. (1) depends upon the relative phase angle ϕ, while the ponderomotive shift of the ionization limit does not.

We have chosen to study the ionization of hydrogen atoms by first and second harmonic fields (1ω-2ω) of the type used by Muller *et al.* [3]. We use an exact time-dependent method, expanding the electronic wave function on a numerical grid and integrating the time-dependent Schrödinger equation for the field in Eq. (1). We calculate ionization rates, ATI spectra, and angular distributions for different choices of the fundamental frequency, intensity, and relative phase. One of our main results is that the phase dependence of multiphoton processes can be used to illustrate the transition from multiphoton to tunneling ionization depending upon the fun-

damental frequency and/or the laser intensity. We believe that these results, though calculated for hydrogen, are generally applicable and that experiments based upon them should be feasible and directly comparable to our predictions, provided that the phase difference between the lasers can be measured. Though we are not aware of any experiments that have successfully measured this phase difference, it may be possible to do so [10]. Control over the phase difference of successive laser pulses has been demonstrated recently [11].

We begin in the next section by reviewing a few features of the calculational method and then discuss the two color field in more detail, especially its symmetry properties. We present detailed results for the ionization of hydrogen by 1064- and 532-nm light at an intensity of 2×10^{13} W/cm^2 and then examine the effect of using shorter-wavelength lasers and higher intensities.

METHOD

We first briefly review our use of time-dependent methods in solving laser-atom problems. Considerably more detail can be found in a recent review article [12]. We consider a hydrogen atom in a classical, linearly polarized field of the form in Eq. (1). Since the fields will have intensities above 10^{13} W/cm^2, we use a nonperturbative method and solve time-dependent Schrödinger equation

$$i\frac{\partial}{\partial t}\psi(\mathbf{r},t)=\left[-\frac{1}{2}\nabla^2-\frac{1}{r}+zf(t)\varepsilon(t)\right]\psi(\mathbf{r},t)\ , \tag{2}$$

where z is the coordinate along the direction of polarization, $\varepsilon(t)$ is given by Eq. (1), and $f(t)$ is the pulse envelope. We use atomic units with $e=\hbar=m=1$. The electronic wave function is expanded in spherical harmonics and the resulting coupled equations are discretized on a radial grid. We begin with the atom in its $1s$ ground state and calculate the time evolution of the wave function using a Peaceman-Rachford propagator [12]. The time step, maximum angular momentum, and size of the radial grid are adjusted as required to achieve convergence. In general, higher angular momenta and larger grids are necessary to handle longer-wavelength fields. Using hydrogen has the advantage that the calculations are exact to within our numerical accuracy.

The choice of pulse shape and radial grid size is dictated by the quantities we wish to calculate. When calculating ionization rates we use a pulse $f(t)$ which rises linearly over several cycles and then remains constant at a value of one for many optical cycles. We use a moderate size radial grid of 100–200 a.u. Since it is unlikely that electrons which have traveled this far from the nucleus can be recaptured, a smooth cosine mask function at the edge of the grid is used to remove any wave function that reaches the boundary. We assume that this corresponds to ionization and calculate ionization rates based upon the rate at which the norm of the wave function decreases on the grid. This yields results which compare well with other accurate methods [12]. The calculation of ATI spectra and energy-resolved angular distributions requires that we use a trapezoidal pulse which rises over a few optical cycles, remains constant for several cycles, and then decreases to zero again. The electron energy and angular distributions are then calculated from the final (field off) wave function via a window operator that we have previously described [13,14]. In order to fully contain the ionizing wave function the numerical grids must be approximately 10 times larger than those used for determining ionization rates. Even with such large grids, we can only integrate Eq. (2) over short pulses. As we will see below, it is still possible to obtain converged, physically meaningful results from such short pulses.

1ω-2ω FIELDS

The shape of the time-varying electric field, shown over three cycles of the fundamental field in Fig. 1, is a strong function of ϕ. The maximum instantaneous field is greatest for $\phi=\pi/2$. This maximum value of $2\varepsilon_0$ is obtained once per cycle while the maximum value of $1.76\varepsilon_0$ is obtained twice per cycle for $\phi=0$. For processes which depend nonlinearly on the peak electric field these differences can lead to very different rates. The two-color field in Eq. (1) can also be rewritten as $2\varepsilon_0\sin(1.5\omega t'-\phi)\cos(0.5\omega t')$ with $t'=t+\phi/\omega$. From this form we note the following symmetries which relate the fields in Fig. 1 to values of ϕ outside the interval 0 to $\pi/2$, ignoring an overall time shift: (i) replacing ϕ with $\phi\pm2\pi$ does not change the time dependence of the field; (ii) replacing ϕ with $\phi\pm\pi$ and z with $-z$ also leaves the time dependence of the laser-atom interaction unchanged; and (iii) replacing ϕ with $-\phi$ and t with $-t$ changes the sign of the field but not its magnitude. In case (ii), the angular distribution of the emitted photoelectrons is reflected through the plane perpendicular to the laser polarization. In case (iii), as we will see below, the change in sign of the phase can lead to completely different ionization rates, angular distributions, and ATI spectra.

Examining Fig. 1 it is obvious that the combination of 1ω-2ω fields can lead to asymmetric ionization, given that for some values of the phase very large fields in the forward or backward direction are not balanced by opposite fields in the next half-cycle. Even for $\phi=0$, when the peak forward and backward fields have the same magnitude, asymmetric ionization is possible since a large peak in the positive direction is followed by a small peak in the negative direction, while the reverse is not true. This dependence on the detailed shape of the electric field over an optical cycle will be demonstrated in the following section. Finally, we note that the time-dependent field formed in a 1ω-3ω experiment are completely symmetric for any value of ϕ.

RESULTS: 1064 nm

We first present results for a hydrogen atom subject to two lasers, one at the fundamental of the Nd:YAG (YAG denotes yttrium aluminum garnet) laser ($\lambda_1=1064$ nm) and the other its second harmonic ($\lambda_2=532$ nm). We calculate the total ionization rate by fitting the decay of the norm of the wave function caused by its absorption at the

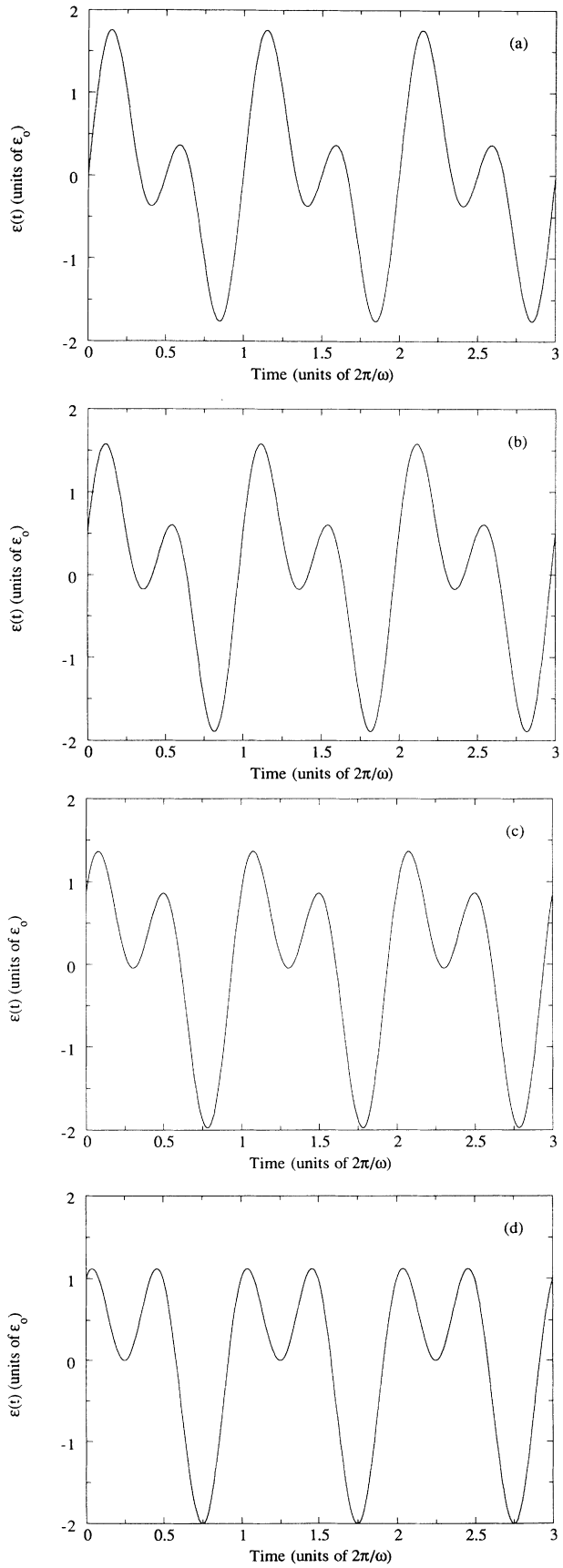

FIG. 1. Time-dependent electric field (in units of ε_0) for (a) $\phi=0$, (b) $\pi/6$, (c) $\pi/3$, and (d) $\pi/2$.

boundaries of our computational box approximately 200 a.u. from the nucleus. We also calculate the amount of ionization in the forward and backward directions by integrating the absorbed flux at the boundaries in the *entire* forward direction ($\theta=0°$–$90°$) or in the *entire* backward direction ($\theta=90°$–$180°$). (Note that Muller *et al.* [3] measured ionization only along one direction of the polarization.) We consider intensities above 1×10^{13} W/cm^2, which are in the nonperturbative regime, and present the emission rates as a function of ϕ, the phase difference between the fields. From our previous work on this system [12] we know that in this intensity range ionization is beginning to enter the tunneling domain for the longer wavelength. Generally speaking, tunneling is expected to dominate the ionization dynamics when the Keldysh parameter [15]

$$\gamma^2=\frac{2\omega^2E_g}{I_0} \tag{3}$$

is ≤ 1. Here ω is the laser frequency, I_0 the intensity, and E_g is the ground-state ionization potential. A transition to the tunneling regime is therefore expected whenever the wavelength becomes sufficiently long, or the intensity becomes sufficiently high. In this limit the electron is more likely to leak through the potential barrier when it is suppressed by the field, as in the dc case, than to absorb enough photons for a direct transition to the continuum.

In Fig. 2 we show the phase dependence of the total ionization probability after 20 cycles, as well as the forward and backward components, at a constant intensity $I_0=c\varepsilon_0^2/8\pi$ of 1×10^{13} and 2×10^{13} W/cm^2. The ionization is greatest for $\phi=\pm\pi/2$, which produces the largest maximum electric field. The total ionization probability has a period of π, and depends only upon the maximum field strength. This is typical of ionization in the tunneling regime. The partial rates (i.e., the forward and backward distributions), however, have a period of 2π and show marked asymmetry. This is true even for $\phi=0$, when the peak forward and backward field strengths are equal. The partial rates show a sensitivity to the detailed shape of the electric field that is not present in the total ionization rate. The emission in the forward direction is the same as in the backward direction for $\phi=\pm\pi$, as expected. There is no connection between the forward and backward emission for $+\phi$ and $-\phi$, other than the observation that the *sum* of the forward and the backward emission is the same for both cases. Therefore an experiment that measures the phase dependence of the total ionization probability for this case must measure the emission in either the forward or backward directions separately over a range of 2π, or in both directions over π.

As the intensity increases, ionization is dominated by tunneling during the interval when the combined fields give the largest amplitude. It might be expected that the forward and backward emission would have their maxima at $+\pi/2$ and $-\pi/2$, respectively, since these produce the maximum forward and backward forces on the electron. Muller *et al.* [3] used this assumption when in-

terpreting the data from their experiment, since they did not measure the absolute phase difference between their lasers. From the partial distributions shown in Fig. 2 it is clear that this assumption is only approximately true. The peak forward-backward emission does occur close to $\pm\pi/2$, and the asymmetry between them grows as the intensity increases. Even at $\phi=0$, though, the emission is not symmetric, as discussed above. In calculations for helium at the same wavelengths but at an intensity of the two fields equal to 5×10^{14} W/cm^2 it was found that over 93% of the electrons were emitted in one direction for $\phi=\pi/2$. This was well into the tunneling regime and is an impressive illustration of a type of coherent control [6].

We next examine the phase dependence of the emitted electron energy distributions. The pulse shape [$f(t)$ in Eq. (2)] consists of a one cycle linear ramp, followed by five cycles of constant intensity and then a one cycle cutoff. The trapezoidal shape allows us to identify the spectrum of emitted energies with the constant intensity portion of the pulse. The ATI spectrum is calculated at the end of the pulse with the fields off. Although this is a very short pulse (about 20 fs), each optical cycle of the fundamental laser corresponds to about 12 orbital periods

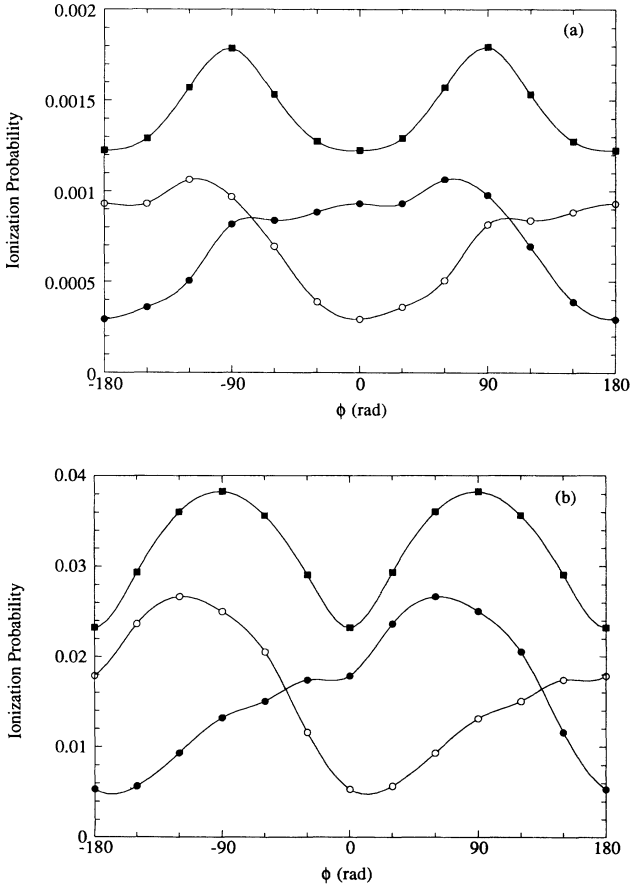

FIG. 2. The total (solid squares) and directional (solid circles, forward; open circles, backward) amount of ionization after 20 optical cycles as functions of the relative phase angle ϕ for (a) $I_0=1\times10^{13}$ W/cm^2, and (b) $I_0=2\times10^{13}$ W/cm^2. The fundamental wavelength is 1064 nm.

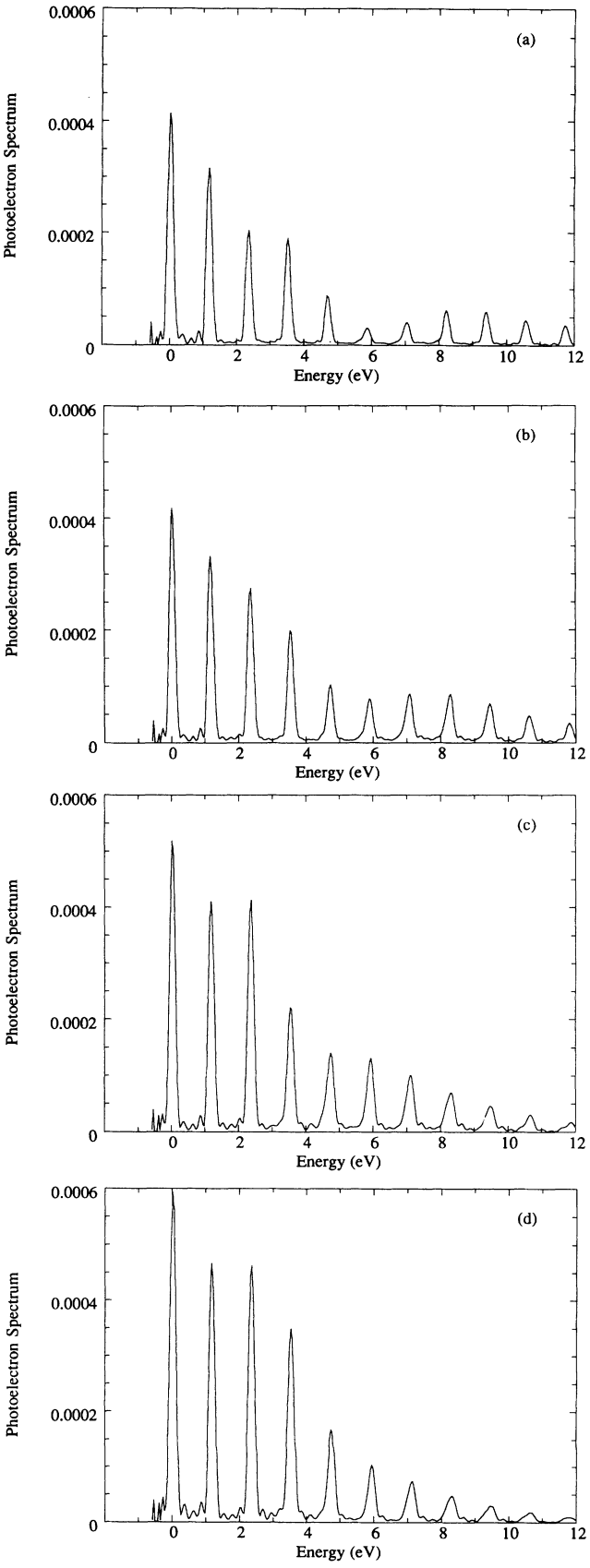

FIG. 3. The emitted electron spectrum for (a) $\phi=0$, (b) $\pi/6$, (c) $\pi/3$, and (d) $\pi/2$ at $I_0=2\times10^{13}$ W/cm^2. The fundamental wavelength is 1064 nm.

for an electron in the hydrogen 1s state. This yields very stable dynamics from cycle to cycle during the constant intensity portion of the pulse and gives us confidence that the results of a longer pulse would not differ significantly from those of this pulse. For example, during each of the five constant optical cycles we observe the same ionization rate (to within about 10%) as we observe with much longer pulses. All of the ATI peaks are broadened by an amount consistent with the spread of photon energies inherent in a finite pulse of this length. The main effect of using a longer pulse would be to further narrow the peaks.

Figure 3 shows ATI spectra for the four fields depicted in Fig. 1. The laser intensity is $I_0=2\times10^{13}$ W/cm^2. The distributions show strong phase dependences as well as evidence of interference effects. The ponderomotive shift, however, is the simple sum of the shifts for the two laser fields and shows no evidence of a phase dependence. These results are consistent with the experiments of Muller *et al.* [3], which found similar phase dependence in the ATI for krypton. Approximate N-photon partial rates can be calculated from these spectra by integrating the area under each peak and dividing by the pulse length. Figure 4(a) shows our results at $I_0=2\times10^{13}$ W/cm^2 for $\phi=\pm\pi/6$. The *partial* rates are quite different although the *total* rates obtained by summing the partial rates are the same. In Fig. 4(b) we compare the partial rates for $\phi=+\pi/3$, $-\pi/3$, and $-2\pi/3$. As expected, the partial rates for $\phi=\pi/3$ and $-2\pi/3$ agree, since they differ only in the direction of the ionization. The $\phi=-\pi/3$ rates are, however, completely different. Again, the sum of the partial rates agree with each other for all three phases shown. Evidently, though excitation to the continuum depends only on the maximum field strength, the distribution of probability over the various continuum states (ATI peaks) depends sensitively on the relative phase of the two laser fields. Muller *et al.* [3] have discussed a model for such two-color ATI spectra in terms of the power spectrum of two color Volkov states. This model reproduces many of the qualitative features shown in Figs. 3 and 4, as well as in the experiments, such as the variation in peak heights with phase angle and the interference effects. This model also predicts, however, that the spectra for $\pm\phi$ will be the same, which is not substantiated by our calculations.

Figure 5 shows angular distributions of the first ATI peak for $I_0=2\times10^{13}$ W/cm^2. The distributions for $\phi=\pi/3$ and $-2\pi/3$ are expected to be mirror images of each other, and they are to within the accuracy of the calculation. The distributions for $\phi=+\pi/3$ and

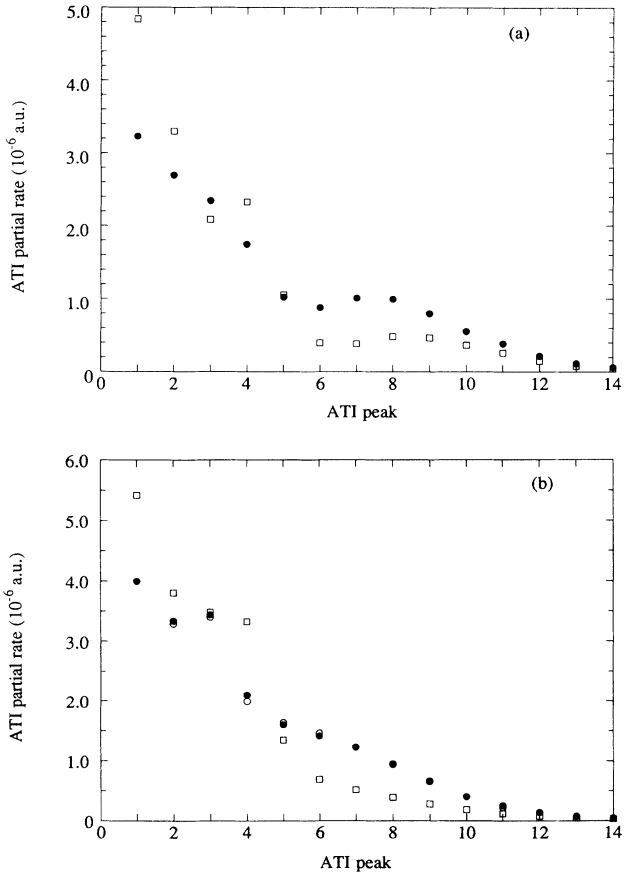

FIG. 4. The ATI partial rates (in a.u.) for $I_0=2\times10^{13}$ W/cm^2. The fundamental wavelength is 1064 nm and the phase angles are (a) $-\pi/6$ (open square) and $+\pi/6$ (solid circle); (b) $-\pi/3$ (open square), $+\pi/3$ (filled circle), and $-2\pi/3$ (open circle).

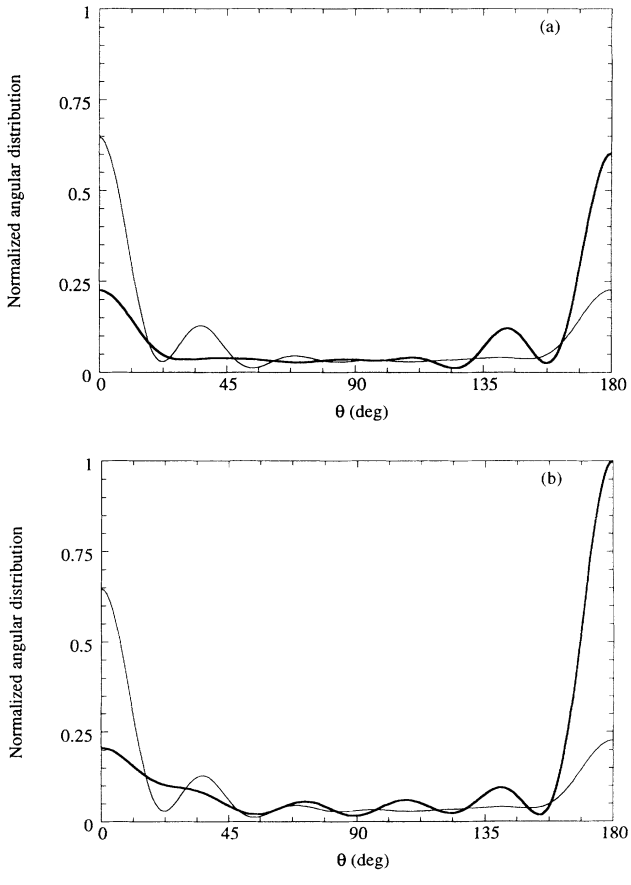

FIG. 5. Angular distributions for the lowest ATI peak at $I_0=2\times10^{13}$ W/cm^2 and $\lambda_1=1064$ nm. The phase angles are (a) $-2\pi/3$ (bold line) and $+\pi/3$ (thin line); (b) $-\pi/3$ (bold line) and $+\pi/3$ (thin line). All of the curves have been normalized to the value of the $\phi=-\pi/3$ data in the forward direction.

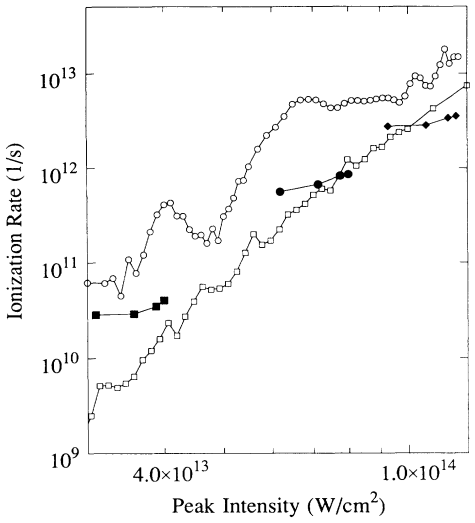

FIG. 6. One- and two-color rates as functions of the peak intensity defined in the text. 1064 nm alone (open squares); 532 nm alone (open circles); 1064+532 nm and $I_0=1\times10^{13}$ W/cm^2 (solid squares); $I_0=2\times10^{13}$ W/cm^2 (solid circles); $I_0=3\times10^{13}$ W/cm^2 (solid diamonds).

$\phi=-\pi/3$ are again quite different, especially close to the axis of polarization. The distributions are strongly peaked along the forward (or backward) direction as expected in the tunneling regime.

We close this section by comparing the total ionization rate for hydrogen subject to one and two color fields. In Fig. 6 we show the total ionization rate for single frequency ionization at 1064 and 532 nm. At the higher frequency strong resonance features are evident. As the intensity increases, the rates for these two frequencies begin to merge, indicating the onset of tunneling. Also shown in the figure are the total rates for two-color ionization as functions of the effective peak intensity corresponding to the square of the phase-dependent peak electric field: $I_{\rm peak}\equiv c\varepsilon_{\rm max}^2(\phi)/8\pi$. We show three cases where the two lasers have intensities $I_0=c\varepsilon_0^2/8\pi$ of 1×10^{13}, 2×10^{13}, or 3×10^{13} W/cm^2. The two color rates fall close to the results for the lower frequency laser at the higher intensities. This is another strong indication that we are in the tunneling regime [16].

RESULTS: SHORTER WAVELENGTHS

We now examine cases where the fundamental laser wavelength is shorter than 1064 nm. Figure 7 shows ATI spectra for $\lambda_1=532$ nm ($\lambda_2=266.5$ nm) and $I_0=2\times10^{13}$ W/cm^2. The spectra for $\phi=0$ and $\pi/2$ exhibit many of the same effects seen with the longer wavelength at this intensity. The peaks display strong variations with the phase angle. The ponderomotive shift is again the simple sum of the shifts for the two lasers at the intensity I_0, with no dependence on the phase angle. The use of shorter wavelengths does, however, lead to important differences. As the wavelength decreases the character of the ionization dynamics begins to be dominated by multiphoton effects. Since ionization occurs by the absorption

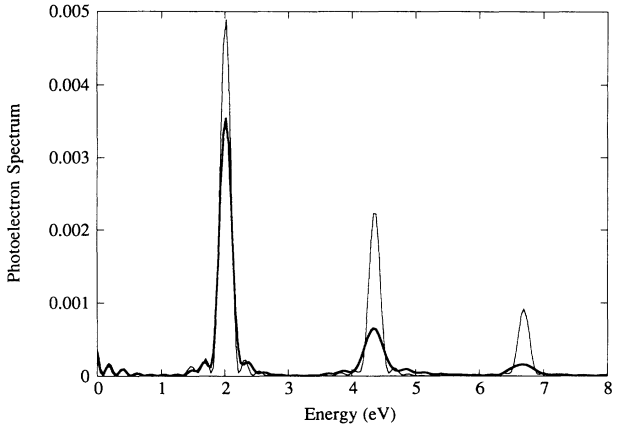

FIG. 7. ATI spectra for $I_0=2\times10^{13}$ W/cm^2 and a fundamental wavelength of 532 nm. The phase angles are 0 (thin line) and $+\pi/2$ (bold line).

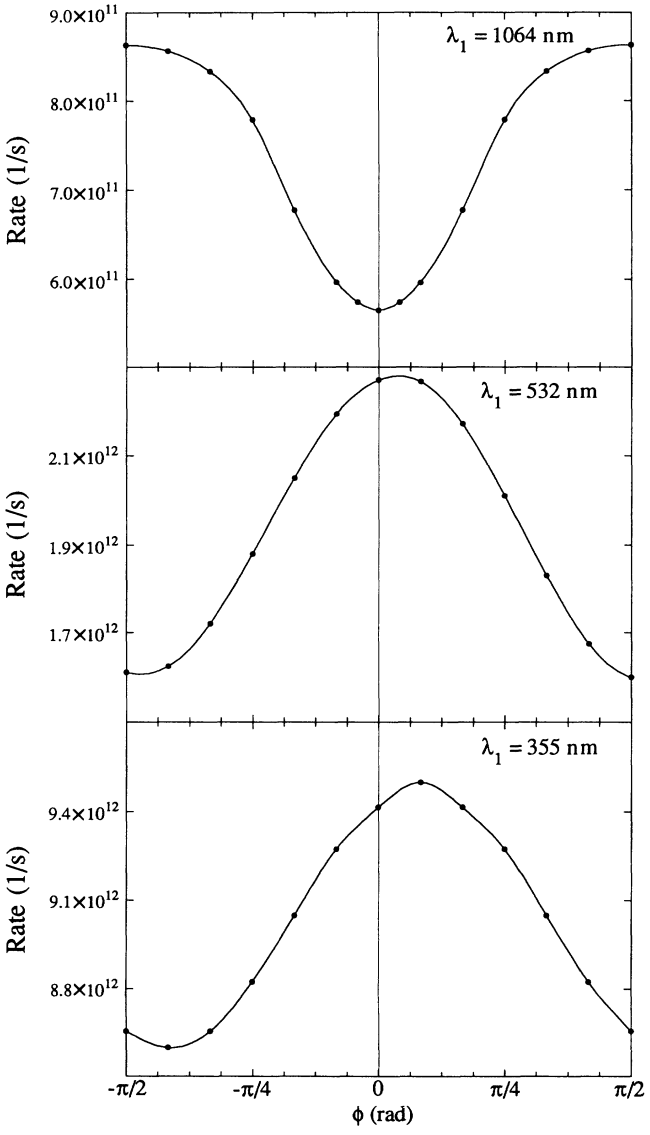

FIG. 8. Total ionization rates (in 1/sec) as a function of phase angle for $I_0=2\times10^{13}$ W/cm^2 and fundamental wavelengths of $\lambda_1=1064$, 532, and 355 nm.

of a smaller number of photons than at 1064 nm the peak electric field becomes less important. This can be clearly seen in Fig. 8, which presents total rates for 1ω-2ω ionization where each laser has an intensity of $I_0=2\times10^{13}$ W/cm^2 and the fundamental wavelengths are $\lambda_1=1064$, 532, or 355 nm. The upper curve repeats the results for the longest wavelength shown earlier. The two lower panels are dramatically different in that the peak rate does not occur for the phase that produces the largest peak electric field. The symmetry with respect to $\phi=0$ is also absent (the total rates now have a periodicity of 2π instead of π). Presumedly, the interference between a few multiphoton excitation pathways, and not simply the peak electric field, influences the total ionization rate. This is responsible for the shift of the peak in the ionization rate away from $\pm\pi/2$ and towards $\phi=0$. The experimental identification of tunneling versus multiphoton ionization requires the measurement of the phase difference between the lasers. The simple assumption that the peak forward or backward ionization rate occurs at $\phi=\pm\pi/2$ is not sufficient to determine this phase, as we demonstrated above.

The wavelength dependence of the angular distributions for the lowest open ATI channel is illustrated in Fig. 9, where distributions are compared for fundamental wavelengths of $\lambda_1=1064$ and 532 nm. The $\lambda_1=532$ nm distributions tend to be broader, more symmetric, and show significant variations at angles away from the polarization axis. The increased structure in the angular distributions at shorter wavelength is consistent with the idea that only a few partial waves contribute to the ATI peak.

As we emphasized earlier, a transition to the tunneling regime is expected whenever the wavelength becomes sufficiently long, or the intensity sufficiently high. Figure 7 illustrates the first of these criteria and the second is illustrated in Fig. 10. We show the total ionization rate for a 1ω-2ω field where λ_1 is held fixed at 660 nm and the intensity is increased from 1 to 3×10^{13} W/cm^2. As the intensity increases the phase dependence recovers the form seen earlier for 1064 nm. By 3×10^{13} W/cm^2 the rate depends almost exclusively on the (ϕ-dependent) peak electric field.

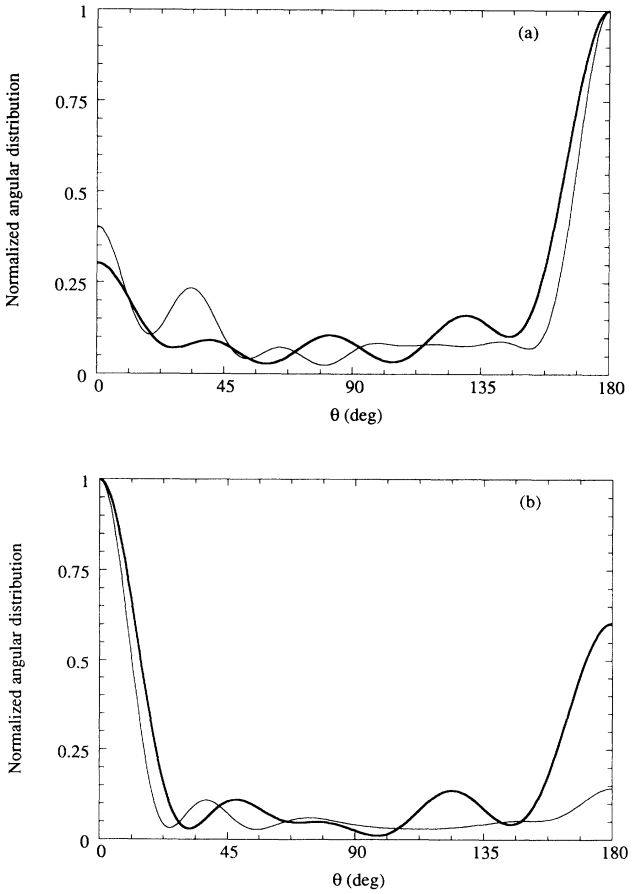

FIG. 9. Angular distributions for $I_0=2\times10^{13}$ W/cm^2 at fundamental wavelengths of 1064 nm (fine line) and 532 nm (bold line) for phase angles of (a) 0 and (b) $+\pi/2$.

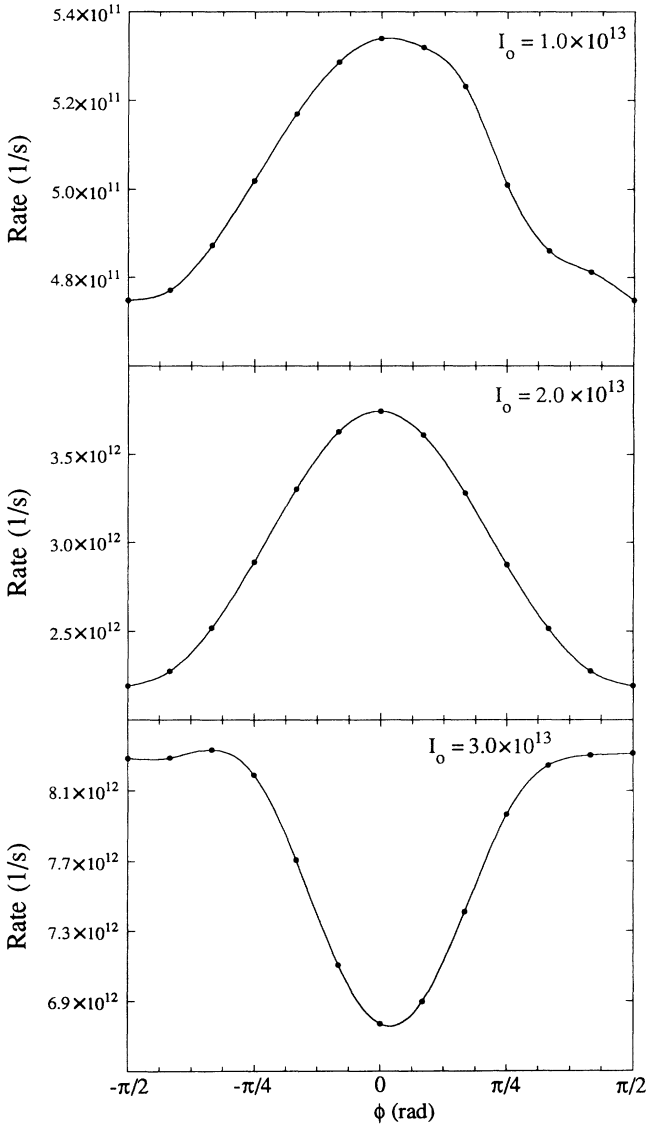

FIG. 10. Total ionization rates (in 1/sec) as functions of phase angle for a fundamental wavelength of $\lambda_1=660$ nm and intensities of $I_0=1$, 2, and 3×10^{13} W/cm^2.

CONCLUSIONS

The preceding results demonstrate that using different wavelengths or intensities in a 1ω-2ω experiment leads to a qualitative change in the ionization dynamics. At longer wavelengths the total ionization rate is determined solely by the peak instantaneous electric field. This is characteristic of tunneling ionization. We emphasize again, however, that all of the various partial rates (i.e., the angular distributions and the magnitudes of the individual ATI peaks) show considerable phase-dependent structure. The phase dependence of the individual ATI peaks, particularly the interference effects in Fig. 3, sharply contrasts with the monotonic (power-law) decline in successive ATI peaks found in earlier one-color calculations at these wavelengths and intensities [13]. This behavior demonstrates that, although the total amount of excitation from the ground state to the continuum is controlled by the peak electric field, the distribution of emitted electrons among the various continuum states is sensitive to the detailed sequence of maxima and minima in the combined electric field during each optical cycle. At shorter wavelengths, excitation takes place via a smaller number of photons and the dependence of the ionization rate on the peak field is weakened. A transition from multiphoton to tunneling ionization also occurs if the intensities of the lasers is increased at a given fundamental wavelength.

We find, in agreement with earlier studies, that a substantial forward-backward asymmetry can be achieved in the ionization signal with a 1ω-2ω field. This effect suggests a strong analogy to the coherent control experiments proposed for molecules with 1ω-3ω fields. Such spatial asymmetry is not possible in a 1ω-3ω experiment since the combined electric field is symmetric with respect to the ordering of successive maxima and minima, although the total ionization signal and differential cross sections can be modulated by changing the relative phase. For this same reason the 1ω-3ω field produces only odd harmonics of the fundamental laser while the 1ω-2ω field produces both odd and even harmonics. Though we have not displayed any results on harmonic production from 1ω-2ω fields, we have found that the individual harmonics show phase dependences similar to that found for the ATI peaks. Also, in agreement with previous theoretical studies, we have found no phase dependence in the positions of the ATI peaks at any wavelength or intensity [5,7].

In summary we have demonstrated a variety of phase-dependent effects in 1ω-2ω multiphoton ionization. The calculations were done on hydrogen at a number of intensities and wavelengths and we feel that these results should hold qualitatively for other atoms as well, in particular the more experimentally accessible ones such as the rare gases. All of the calculations were done with equal laser intensities for both fields and this is probably the optimal arrangement for demonstrating the interference effects we have discussed. When the lasers have very different intensities the ionization will be dominated by one or the other wavelength. These calculations strongly support further 1ω-2ω experiments both at shorter wavelengths and with increased angular resolution. They also highlight the additional information which can be gained by measuring the relative phase between the lasers.

ACKNOWLEDGMENTS

This work has been carried out under the auspices of the U.S. Department of Energy at the Lawrence Livermore National Laboratory under Contract No. W-7405-ENG-48. Partial support has been provided to K.J.S. by the National Science Foundation Grant No. PHY90-14797.

[1] H. G. Muller, H. B. van Linden van de Heuvell, and M. J. van der Wiel, J. Phys. B **19**, L733 (1986).
[2] D. Normand, L. A. Lompre, A. L'Huillier, J. Morellec, M. Ferray, J. Lavancier, G. Mainfray, and C. Manus, J. Opt. Soc. Am. B **6**, 1513 (1989).
[3] H. G. Muller, P. H. Bucksbaum, D. W. Schumacher, and A. Zavriyev, J. Phys. B **23**, 2761 (1990).
[4] C. Chen and D. S. Elliot, Phys. Rev. Lett. **65**, 1737 (1990).
[5] A. L'Huillier, L. A. Lompre, D. Normand, X. Tang, and P. Lambropoulos, J. Opt. Soc. Am. B **6**, 1790 (1989).
[6] A. Szöke, K. C. Kulander, and J. N. Bardsley, J. Phys. B **24**, 3165 (1991).
[7] M. Dorr and R. Shakeshaft, Phys. Rev. A **40**, 459 (1989).
[8] M. Shapiro, J. W. Hepburn, and P. Brumer, Chem. Phys. Lett. **149**, 451 (1988).
[9] R. Trainham, G. H. Fletcher, N. B. Mansour, and D. J. Larson, Phys. Rev. Lett. **59**, 2291 (1987).
[10] P. H. Bucksbaum (private communication).
[11] N. F. Scherer, A. J. Ruggiero, M. Du, and G. R. Fleming, J. Chem. Phys. **93**, 856 (1990).
[12] K. C. Kulander, K. J. Schafer, and J. L. Krause, *Atoms in Intense Radiation Fields,* edited by M. Gavrila (Academic, New York, in press).
[13] K. J. Schafer and K. C. Kulander, Phys. Rev. A **42**, 5794 (1990).
[14] K. J. Schafer, Comput. Phys. Commun. **63**, 427 (1991).
[15] V. L. Keldysh, Zh. Eksp. Teor. Fiz. **47**, 1945 (1964) [Sov. Phys.—JETP **20**, 1307 (1965)].
[16] Several authors have discussed the tunneling picture of ATI in the extreme low-frequency limit. See, for example, T. F. Gallagher, Phys. Rev. Lett. **61**, 2304 (1988); P. B. Corkum, N. H. Burnett, and F. Brunel, *ibid.* **62**, 1259 (1989); G. A. Ruff, K. M. Dietrick, and T. F. Gallagher, Phys. Rev. A **42**, 5648 (1990).